Biointerphases (2012) 7:28
DOI 10.1007/s13758-012-0028-8

ARTICLE

Platelet Activation Profiles on TiO_2: Effect of Ca^{2+} Binding to the Surface

Swati Gupta · Ilya Reviakine

Received: 31 December 2011 / Accepted: 15 March 2012 / Published online: 24 April 2012

Abstract Surface ion equilibrium is hypothesized to play an important role in defining the interactions between foreign materials and biological systems. In this study, we compare two surfaces with respect to their ability to activate adhering platelets. One is a commonly used implant material TiO_2, which binds Ca^{2+}, and the other one is glass, which does not. We show, that in the presence of Ca^{2+}, TiO_2 acts as an agonist, activating adhering platelets and causing the expression on their surface of two well-known activation markers, CD62P (P-selectin) and CD63. On the contrary, in the absence of Ca^{2+}, platelets adhering on TiO_2 express only one of the two markers, CD63. Platelets adhering on glass, as well as platelets challenged with soluble agonists in solution, express both markers independently of whether Ca^{2+} is present or not. The expression of CD62P and CD63 is indicative of the exocytosis of the so-called α- and dense granules, respectively. It is a normal response of platelets to activation. Differences in the expression profiles of these two markers point to differential regulation of the exocytosis of the two kinds of granules, confirming the recent notion that platelets can tune their microenvironment in a trigger-specific fashion.

Electronic supplementary material The online version of this article (doi:10.1007/s13758-012-0028-8) contains supplementary material, which is available to authorized users.

S. Gupta · I. Reviakine (✉)
Biosurfaces Unit, CIC BiomaGUNE (Centro de Investigación Cooperativa en Biomateriales), Paseo Miramón 182, 20009 Donostia, San Sebastián, Spain
e-mail: IReviakine@cicbiomagune.es

S. Gupta · I. Reviakine
Department of Biochemistry and Molecular Biology, University of the Basque Country, 48940 Leioa, Spain

1 Introduction

The interplay between surface physico-chemical properties of materials and the biological response they elicit is an active area of research [1]. The role of interfacial ion equilibrium in this process is an aspect that has not received sufficient attention despite the recognition of its importance [1]. In this context, titania–Ca^{2+} interactions represent an interesting example. Titania (TiO_2) is a relatively inert and stable material responsible for the favorable, if poorly understood, biocompatibility properties of titanium (Ti), which is used in the production of various implants—stents, heart valve housings, dental prostheses and other osseoimplants [2–4]. Titania interactions with Ca^{2+} are manifested in terms of changes of several surface properties, such as the isoelectric point (IEP, the pH at which proton dissociation from the surface is balanced by adsorption and the surface charge is neutralized) and ζ-potential: the IEP of TiO_2 is shifted in the presence of calcium to higher pH [5–8], and its ζ-potential is inverted at a near-physiological Ca^{2+} concentration of $\sim$3 mM at physiological pH [8]. These changes can be interpreted in terms of adsorption of Ca^{2+} ions at the oxide surface; this is the so-called "chemical" interpretation. For a detailed discussion of the chemical versus physical interpretation of the charge reversal phenomena, the reader is referred to Lyklema et al. [9], while IEP shifts are discussed in detail in Hunter et al. [10].

In simplest terms, Ca^{2+} adsorption to the surface will change the balance of interactions between the surface and the material (proteins, lipids, cells) adsorbing or adhering to it. Indeed, there is some evidence suggesting that Ca^{2+} adsorption to titania affects TiO_2-protein interactions [11]. Furthermore, on TiO_2, Ca^{2+} elicits a clear response in terms of lipid behavior in phosphatidyl serine (PS)-containing liposomes and supported lipid bilayers—response

that is absent on substrates such as silica or glass [12–15]. Interactions of Ca^{2+} with silica are not manifested by the ζ-potential reversal [16], and at neutral pH the fraction of adsorbed Ca^{2+} ions is quite small [17]. For more details, see Figure S1 in the supporting information. In view of these observations, we hypothesized that the behavior of more complex biological systems on TiO_2 would also be affected by the TiO_2–Ca^{2+} interactions. In order to demonstrate that these interactions have an effect on a biological system, we chose to investigate platelets, because of a clearly identifiable response in terms of activation, and their relevance to material biocompatibility.

Platelets are anuclear 3–4 μm cell fragments that circulate in the blood, scouring the vascular bed for sites of injury, where they become activated. Activated platelets adhere to each other and to the injured tissue, forming a platelet plug, catalyzing coagulation cascade reactions that culminate in fibrin production and clot formation, and coordinate the subsequent inflammatory response and wound healing processes [18–22]. Platelets achieve these functions by releasing and expressing on their surface a variety of soluble and membrane factors—lipids, proteins, and small molecules—that are stored internally in the quiescent platelets. Examples of membrane factors include the phospholipid phosphatidyl serine (PS), which catalyzes the assembly of the coagulation cascade proteins [18, 23, 24], transmembrane protein markers such as CD62P (P-selectin) and CD63 that are characteristic of the exocytosis of the α- and dense storage granules, respectively [25], and integrin GPIIb/IIIa, the active form of which is responsible for the adhesion events [20, 26–31]. Expression of these factors is a useful measure of platelet activation [20, 32, 33].

Contact with artificial surfaces also activates platelets, leading to thrombosis [34, 35], which can be successfully managed with anticoagulants to some extent. However, complications still arise despite the anticoagulant therapy [34]. This is a well-known problem for the development of blood-compatible biomaterials and considerable research efforts are focused on the discovery and development of materials with minimal procoagulatory properties [34, 35]. On the other hand, blood coagulation at surfaces of osseoimplants is beneficial for implant integration. Because of its importance, interactions between whole blood, or its components, and various biomaterials, has been extensively studied [34–40]. Quite a few of these studies focused specifically on TiO_2 [30, 41–51]. There is an overall understanding of the sequence of events, viz., protein adsorption—platelet activation—thrombosis, and it is established that surface protein adsorption and the dynamics of the protein-adsorbed films play a major role in the process of platelet activation by foreign materials [34, 42, 52], although direct surface effects have also been described [26, 41]. However, the nuances of these processes remain poorly understood; in particular, detailed, multifactorial studies of platelet activation by surfaces are hard to come by. There is a distinct lack of suitable biophysical models that would allow the principles underlying these interactions to be elucidated. For this reason, in our study we focus on the purified platelets and on identifying a clear cause-and-effect relationship between surface ion binding and platelet response. We use the expression of different platelet activation markers to elucidate the effect of surfaces such as TiO_2 and glass on the platelets under different ionic conditions. We demonstrate that the pattern of activation marker expression in platelets interacting with TiO_2 depends on whether Ca^{2+} is present or not. This effect is absent in platelets adhering on glass as well as in platelets challenged with agonists in solution.

2 Results

2.1 Platelet Isolation and Purification

Platelets were isolated from human whole blood collected by venipuncture into sodium citrate anticoagulant. In order to establish a clear cause-and-effect relationship between Ca^{2+}–TiO_2 interactions and platelet activation at the TiO_2 surface, we purified platelets from the plasma proteins. Purification was done by centrifugation, after Watson et al. [53] with modifications. Protein concentration in our samples was $\sim 0.05 \pm 0.01$ mg/ml, compared to ~ 130 mg/ml in the blood plasma.

Prior to the surface experiments, platelet behavior in solution was analyzed by flow cytometry to ensure their purity, minimal activation, and appropriate response to agonists [53–56]. The results of this analysis are shown in Fig. 1. They confirm that freshly isolated platelets are not contaminated by other cells and do not express activation markers such as CD62P, CD63, active form of GPIIb/IIIa, or phosphatidyl serine (PS). CD62P and CD63 are indicative of the exocytosis of α- and dense granules, respectively, that occurs in response to activation [25]. GPIIb/IIIa is a constitutively expressed platelet surface integrin that changes conformation upon activation, and the procoagulant phospholipid PS was already discussed above [18, 20, 23–25, 53–56]. Stimulation with soluble agonists (PMA or TRAP) lead to the expression of these markers (Fig. 1, Figure S2 in the Supporting Information). Consistent with previous findings, CD62P and CD63 expression did not depend on the presence of the extracellular Ca^{2+} [56–58]. GPIIb/IIIa activation and the detection of exposed PS with annexin A5 require extracellular Ca^{2+} (Fig. 1) [54, 59]. Only platelets that were not activated upon isolation but responded to the agonists as shown in Fig. 1 were used in subsequent experiments.

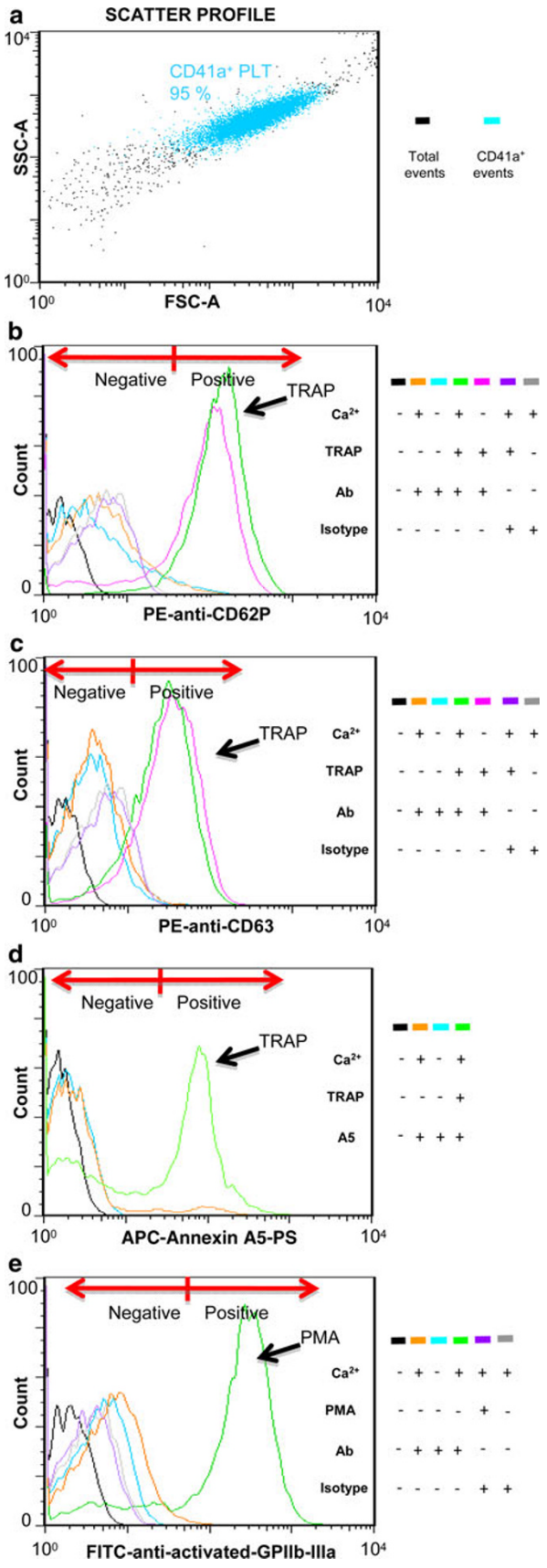

Fig. 1 Flow cytometry analysis of purified platelets. Platelets isolated from sodium citrate-anticoagulated blood were re-suspended in a nominally Ca^{2+}-free buffer and analyzed by flow cytometry [33, 53, 55, 56, 82, 83]. Results of one representative experiment are shown as percentages of positive events out of a total of 10,000 events are shown on the plots. Average values from several experiments are shown in Figure S2 in the Supporting Information. **a** The scatter profile shows one population of cells, 95 % of which stained positive for the platelet-specific marker CD41a (platelet transmembrane glycoprotein GPIIb). This is consistent with what is expected of isolated quiescent platelets that are free of contaminants such as erythrocytes and white blood cells [56, 82, 83]. Platelets stain positive for CD62P (**b**) and CD63 (**c**) upon addition of 70 μM TRAP (*green and pink histograms*) but negative in its absence (*orange and turquoise histograms*). Expression of CD62P and CD63 in TRAP-activated platelets is independent of the extracellular Ca^{2+}: the *pink* (absence of Ca^{2+}) and the *green* (presence of Ca^{2+}) histograms nearly overlap; this is consistent with previous findings [56, 57]. Isotype controls are negative in the presence and in the absence of TRAP (*light purple and grey*). Sample auto-fluorescence recorded in the absence of antibodies is shown in *black*. **d** Platelets expose PS upon activation with 70 μM TRAP as judged by the binding of APC-labeled annexin A5 in the presence of extracellular calcium (*green histogram*). Platelets that were not activated with TRAP do not expose PS (*turquoise histogram*) even when Ca^{2+} is present (*orange histogram*). Annexin A5 binding is Ca^{2+}-dependent; therefore, it is not possible to check whether PS is expressed on the surface of TRAP-activated platelets in the absence of Ca^{2+} with this reagent. *Black* sample auto-fluorescence in the absence of APC-annexin A5. **e** Platelets activated with 10 μM PMA express the active form of GPIIb/IIIa, as judged by the binding of PAC1 antibody in the presence of Ca^{2+} (*green histogram*) [54, 82]. No binding is detected in platelets that were not activated by PMA (*orange and turquoise histogram*). The inactive-to-active conformation change in GPIIb/IIIa is Ca^{2+}-dependent. The Ca^{2+} requirement for PAC1 antibody binding is well-established in the literature and was not tested in our experiments [53, 83, 86]. Isotype controls are negative in the presence and in the absence of PMA (*light purple and grey*)

2.2 Expression of the Activation Marker CD62P Depends on the Extracellular Ca^{2+} in Platelets Adhering on TiO_2, but not on Glass

Freshly isolated, purified platelets were allowed to interact with freshly cleaned, bare glass surfaces or with TiO_2-coated glass surfaces in a Ca^{2+}-free buffer. They adhered and spread on both surfaces (Fig. 2). Both the numbers of adhering platelets and the degree of their spreading were similar on glass and on TiO_2. In both cases, more platelets adhered after 3 h than after 10 min. Some of the platelets adhering on TiO_2 after 3 h were not spread (Fig. 2a-v and Figure S3 in the Supporting Information). The numbers of adhering platelets and their degree of spreading are shown in Table S3 and Figure S3 in the Supporting Information.

On glass, adhering platelets expressed CD62P and CD63 markers, signalling their activation (Fig. 2a-i, iv, b-i, iii). Activation was already noted in many of the platelets incubated with glass for 10 min (Fig. 2a-i, b-i), when platelets were well-separated. Incubation for 3 h led to a

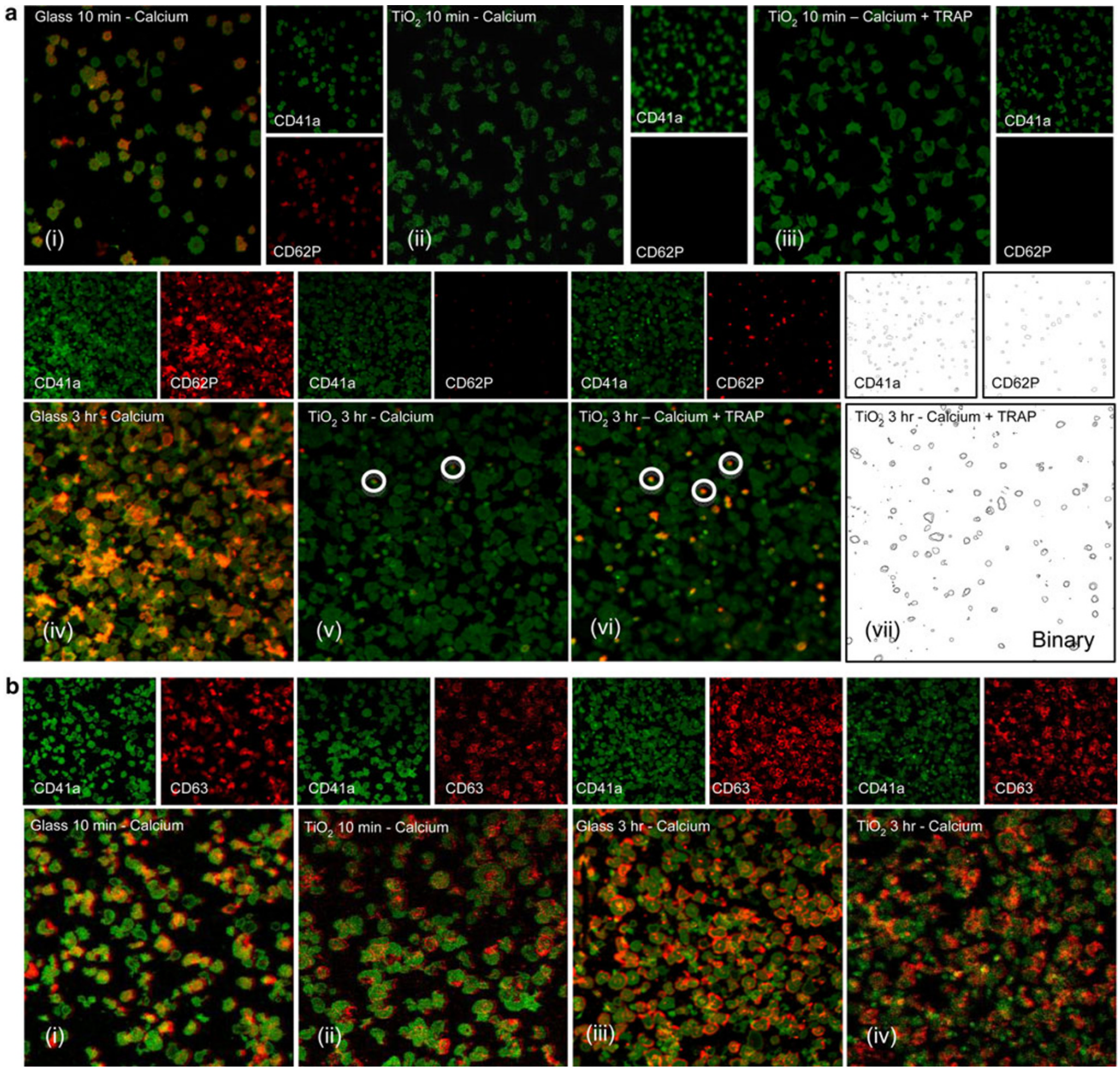

Fig. 2 Platelet activation profiles on titania and glass in the calcium-free buffer. Platelets were incubated with TiO_2-coated or bare glass cover slips for 10 min or for 3 h in a nominally Ca-free buffer and extensively washed with the same buffer. Platelets that remained on the surface were incubated with the following antibodies and observed in the confocal microscope: **a** anti-CD41a (*green*) and anti-CD62P (α-granule marker; *red*); **b** anti-CD41a (*green*) and with anti-CD63 (dense granule marker; *red*). **a** Platelets incubated on glass stain positive with both CD41a and CD62P, showing clear evidence of activation after 10 min (*i*) and after 3 h (*iv*). Platelets incubated on TiO_2 show no evidence of activation (no staining with CD62P) after 10 min even in the presence of TRAP (*ii*, *iii*). Platelets incubated on TiO_2 for 3 h do show evidence of activation (*v*, *vi*), however, the co-localization analysis [*vii*; *white circles* in (*v*) and (*vi*)] shows that it is the second (non-spread) population of platelets that expresses CD62P. The spread platelets from the first layer do not express CD62P even after 3 h of incubation on TiO_2 and in the presence of TRAP (*vi*). **b** CD63 is expressed on platelets adhering to either surface after 10 min or 3 h

near-confluent layer of activated platelets on the surface (Fig. 2a-iv). These observations are consistent with previous reports of platelet activation on glass in the absence of anticoagulants, both in the presence and in the absence of plasma proteins [60–63].

Crucially, platelets incubated for 10 min on TiO_2 in a Ca-free buffer did not express CD62P (Fig. 2a-ii) or respond to TRAP (Fig. 2a-iii). Addition of Ca^{2+} after adhesion did not activate these platelets and did not restore their ability to respond to TRAP (Figure S4 in the

Supporting Information). After 3 h of incubation in a Ca-free buffer, there were platelets on TiO_2 that did express CD62P and responded to TRAP, but these were the non-spread platelets (Fig. 2a-v–vii).

Platelets adhering on TiO_2 in the absence of Ca^{2+} did express the dense granule marker CD63 (Fig. 2b), suggesting that the exocytosis of the α-granules and dense granules is differentially regulated.

In the presence of 2 mM Ca^{2+}, platelets adhered, spread, and expressed CD62P both on TiO_2 and on glass, after 10 min and after 3 h (Fig. 3a). More platelets adhered to the surface in the presence of Ca^{2+} than in its absence (c.f. Figs. 2a-i, ii and 3a-i, ii; see Table S3 in the Supporting Information), and after 10 min of incubation, platelets adhering in the presence of Ca^{2+} spread to a greater extent on both surfaces (Figure S3 in the Supporting Information). Furthermore, there was a difference in the distribution of the integrin GPIIb/IIIa. It appeared to be concentrated at the periphery of the spread platelets in presence of Ca^{2+} (Fig. 3a), while it was uniformly distributed in its absence (Fig. 2). The significance of this difference is not clear. Such non-uniform staining has been previously observed with this protein in activated platelets [64], though platelets adhering on glass are reported to have a centrally located pool of GPIIb/IIIa surrounded by concentric rings [20].

2.3 Chelating Intracellular Ca^{2+} Affects the Expression of Both Activation Markers (CD62P and CD63)

To further elucidate the role of calcium in the differential platelet activation at surfaces, the platelet cytoplasmic calcium was chelated by incubating them with BAPTA-AM. BAPTA-AM is an ester that can freely cross the plasma membrane but is hydrolyzed once inside the platelet. The resulting membrane-impermeable acid acts as a chelator of cytoplasmic Ca^{2+} [65, 66]. Figure 3b shows that platelets in solution loose their ability to express CD62P and CD63 in response to stimulation with TRAP if their cytoplasmic calcium is chelated by BAPTA-AM. This is expected, because both processes require the rise in cytosolic Ca^{2+} [20]. Similarly, chelation of intracellular Ca^{2+} significantly reduced the ability of platelets adhering on glass to express these two markers (c.f. Figs. 3c-i, iii, with Fig. 2a-i, iv for CD62P and Fig. 3c-v, vii with Fig. 2b-i, iii for CD63). BAPTA-AM treatment also significantly reduced the extent of expression of CD63 in platelets interacting with TiO_2 (c.f. Figs. 3c-vi, viii with Fig. 2b-ii, iv). Since CD62P is not expressed in platelets interacting with TiO_2 in the absence of extracellular Ca^{2+}, BAPTA-AM treatment had no further effect on the expression of this marker (Fig. 3c-ii, iv). Chelation of intracellular Ca^{2+} did reduce the extent of platelet spreading on TiO_2 and to a lesser extent on glass (Figure S3 in Supporting Information). A similar effect has previously been observed on polystyrene [67].

3 Discussion

In the presence of the extracellular calcium, TiO_2 acts as an agonist, activating adhering platelets, as judged by the expression of the α- and dense granule markers CD62P and CD63. Its effect is similar to that of glass or of soluble agonists such as TRAP. In the absence of the extracellular calcium, the effect of TiO_2 on the adhering platelets is markedly different from that of the other agonists: platelets adhering on TiO_2 express CD63 but not CD62P, while platelets adhering on glass, or challenged with agonists in solution, express both markers. These trends are visible in the images of individual experiments shown in Figs. 2 and 3, and are also apparent in the average data from different experiments shown in Fig. 4.

The simplest mechanism behind this effect would be that TiO_2, because of its affinity for Ca^{2+} [5–8], acts as a Ca^{2+}-chelator: it could deplete intracellular Ca^{2+}, the way BAPTA-AM does, and/or remove structurally important ions from the outer surface of the platelet membranes, the way EDTA does [83]. This mechanism does not account for our observations, however: firstly, we see a clear difference between the effect of the intracellular Ca^{2+} chelator BAPTA-AM and the effect of TiO_2. The former affects the expression of both markers, while the latter concerns only CD62P. Secondly, chelation of the extracellular Ca^{2+} by EDTA or citrate does not prevent the expression of either of the two markers in platelets challenged with various agonists [68, 69]. In other words, platelets must directly sense differences in the surface properties between TiO_2 in the presence and in the absence of Ca^{2+}.

It should be pointed out that we observed two kinds of platelets on both surfaces. We refer to them as spread and non-spread. The spread platelets are present after 10 min and have extensive platelet-surface contacts but limited platelet–platelet contacts (Fig. 2a i, ii). They persist on the surface after 3 h. The non-spread platelets appear at longer times and are observed after 3 h (Fig. 2a iv–vii). They have limited contact with the substrate but appear to be in contact with other platelets. Most likely, these two populations arise simply due to the surface exclusion effects: at the initial stages of adsorption, there is sufficient space for the adhering platelets to spread, but as the surface becomes covered, the adsorbing platelets can no longer spread out as they are limited by the presence of other platelets. There is a difference in the behavior of the two populations on TiO_2 in the absence of Ca^{2+}: the non-spread platelets expressed

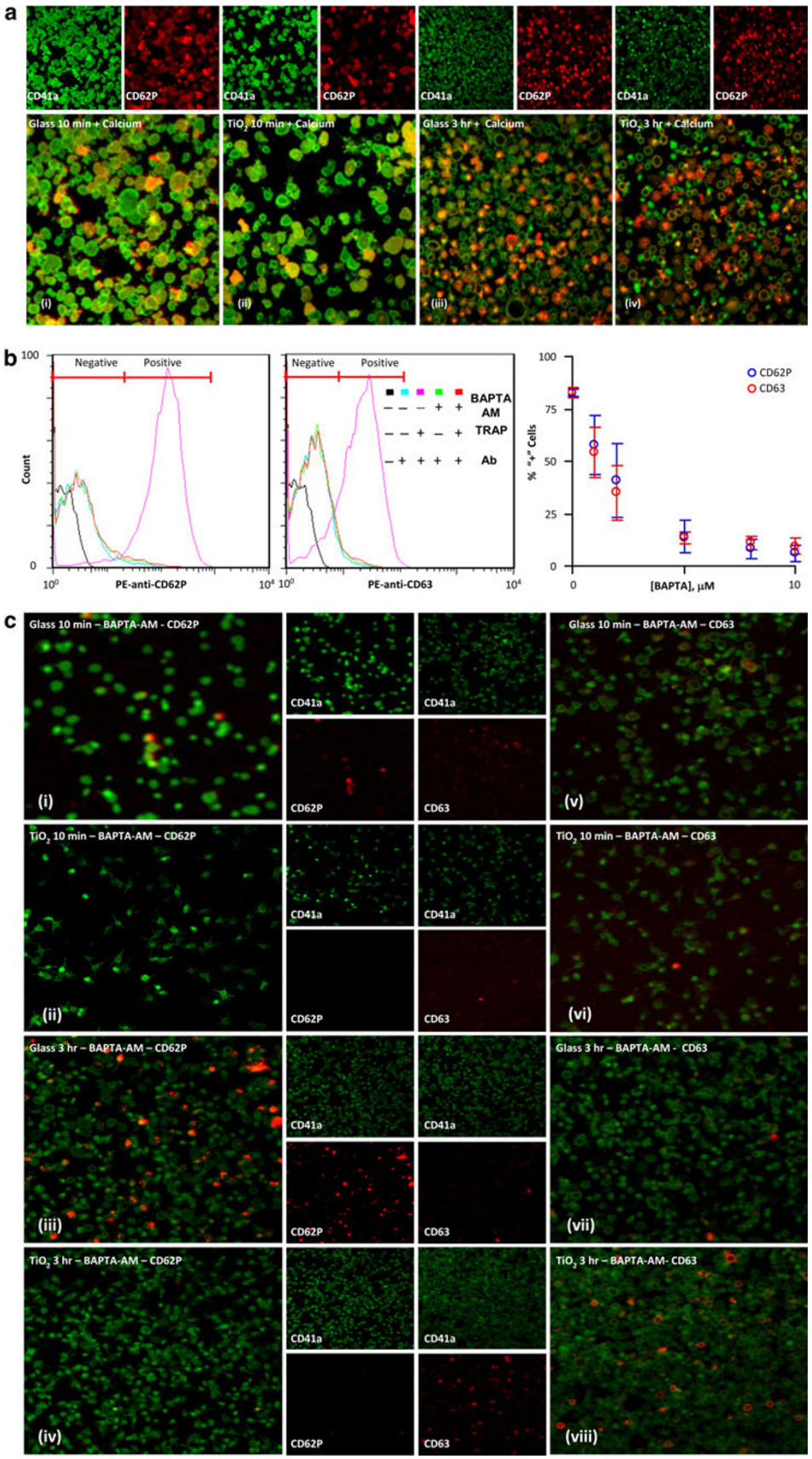
a
CD41a
CD62P
Glass 10 min + Calcium
TiO2 10 min + Calcium
Glass 3 hr + Calcium
TiO2 3 hr + Calcium
(i)
(ii)
(iii)
(iv)
b
Negative
Positive
Count
PE-anti-CD62P
PE-anti-CD63
BAPTA AM
TRAP
Ab
% "+" Cells
[BAPTA], μM
CD62P
CD63
c
Glass 10 min – BAPTA-AM - CD62P
Glass 10 min – BAPTA-AM – CD63
TiO2 10 min – BAPTA-AM – CD62P
TiO2 10 min – BAPTA-AM – CD63
Glass 3 hr – BAPTA-AM – CD62P
Glass 3 hr – BAPTA-AM - CD63
TiO2 3 hr – BAPTA-AM – CD62P
TiO2 3 hr – BAPTA-AM- CD63
(v)
(vi)
(vii)
(viii)

◀ **Fig. 3** Extracellular versus intracellular Ca^{2+} in platelet activation on TiO_2 and on glass. **a** Platelets isolated in the calcium-containing buffer (2 mM $CaCl_2$) were incubated with bare (*i* and *iii*) or TiO_2-coated (*ii* and *iv*) glass cover slips for 10 min (*i* and *ii*) and 3 h (*iii* and *iv*), followed by extensive washing with the same buffer and incubation with antibodies specific against the platelet marker CD41a (*green*) and activation marker CD62P (P-selectin, *red*). The expression of P-selectin was observed on the majority of platelets both after 10 min and 3 h of contact with either surface. **b** *Histograms* Platelets isolated in the nominally calcium-free buffer were treated with BAPTA-AM (100 μM) for 30 min to chelate the intracellular Ca^{2+}, and analyzed by flow cytometry. They do not express CD62P (*left, red*) or CD63 (*right, red*) upon stimulation with an agonist (TRAP). Untreated stimulated platelets do (*pink*). Non-stimulated platelets do not express CD62P or CD63 independently of the BAPTA-AM treatment (*green and turquoise*). Sample auto-fluorescence recorded in the absence of antibodies is shown in *black*. Plot: % of CD62P (*blue*)- and % of CD63 (*red*)- positive platelets as determined with flow cytometry by analyzing the histograms such as those shown on the *left* upon stimulation with 70 μM TRAP as a function of the BAPTA-AM concentration. Each *point* represents an average of six experiments, three of which were performed in the Ca-free HEPES buffer and three—in the citrate buffer; no differences were detected between the two sets. This plot demonstrates that the chelation of intracellular Ca^{2+} affects the expression of both of these markers in the same way. **c** BAPTA-AM treated platelets were incubated with the glass and TiO_2 surfaces and analyzed for CD41a (*green*) and CD62P or CD63 (*red*) expression by confocal microscopy. No spreading was observed on either of the two surfaces after 10 min or after 3 h of incubation (see Figure S3 in Supporting Information). Some CD62P expression is evident in platelets incubated on glass (*i* and *iii*). On the contrary, no CD62P expression was observed in platelets incubated on TiO_2 (*ii* and *iv*). Some CD63 expression is evident on both glass (*v* and *vii*) and TiO_2 (*vi* and *viii*) surfaces

some CD62P and responded to TRAP, while the spread platelets did not (Fig. 2a-v, vi). This observation may appear counterintuitive, because platelet spreading and activation are usually coupled [20, 70, 71]. This is not always the case, however: non-spread, activated platelets have been observed before. In platelets adhering on collagen, they appear in the very early stages of the adhesion process and contribute to thrombus formation through platelet–platelet interactions [31]. Broberg et al. [72] shows several examples where platelet spreading and activation (as judged by the expression of CD62P) are not correlated. Similarly Pandey et al. [73] show that low concentrations of lysophosphatidic acid induce platelet shape changes but not granule secretion. The difference in behavior between the spread and non-spread platelets we observe on TiO_2 in the absence of Ca^{2+} appears to be related to the platelet-surface contact area or to the platelet–platelet interactions.

One of the consequences of platelets' ability to sense differences in TiO_2 surface properties is the differential expression of the α- and dense granule markers that we observe on titania in the absence of Ca^{2+}. As early as 1988, Kang et al. [39] showed that exocytosis of the dense granules, as judged by the serotonin release, correlated with the number of platelets adhering to the surface, while the release of α-granules, as judged by the release of β-thromboglobulin, was selective in regards to the surface properties and peaked in a particular range of surface wetability values they tested. Rhodes et al. [37] in 1994 also showed that granule release was differentially induced by the different surfaces and flow regimes, and Taylor et al. [74] demonstrated that the level of expression of α- and dense granule markers depends on the agonist concentration and strength differently. These studies were done with whole blood and PrP. Our observation of the differential granule release is therefore not restricted to the purified platelets but is a manifestation of a more general aspect of platelet behaviour, that could allow them to tune the microenvironment at the wound site [19]. Molecular mechanism behind this behavior is most likely rooted in the different regulatory machinery associated with the secretion of the two types of granules: it is reported that the secretion of α- and dense granules is regulated by two different Rab-GTPases (Rab4A and Rab27A) [75–78] and is affected differently by actin polymerization inhibitors [57, 77]. α-granules themselves appear to contain subpopulations, the release of which is regulated differentially [79], further supporting the idea of platelets tuning the environment of the wound. This is an active area of research [19]. However, it is at this point not clear how this differential regulation is achieved: what are the stimuli and how are they transmitted to the different granules. This complicates further interpretation of our observations at the molecular level, but does provide an interesting starting point for further investigations. In the context of the possible applications, surface-induced and surface-charge regulated differential granule release can be used for controlled molecule release from platelets, e.g., by nanoparticles, or implants in drug delivery applications [80].

4 Materials and Methods

4.1 Blood Collection

Blood collection was organized by the Biobanco Vasco para la Investigación (Basque Biobank for Research, Galdakao, Spain) and performed with informed consent according to the appropriate legal and ethical guidelines. Donors were healthy volunteers without the history of exposure to medication (such as aspirin) or exposure to alcohol in the 2 weeks prior to collection. 10 ml of blood was collected by venipuncture with a 21 gauge needle into sodium citrate anticoagulant (two 5 ml glass Vacutainer® tubes, Becton Dickenson, Madrid, Spain, from each donor) and stored at 37 °C. First 2 ml of blood was discarded during the collection to avoid platelet activation by residual thrombin [53].

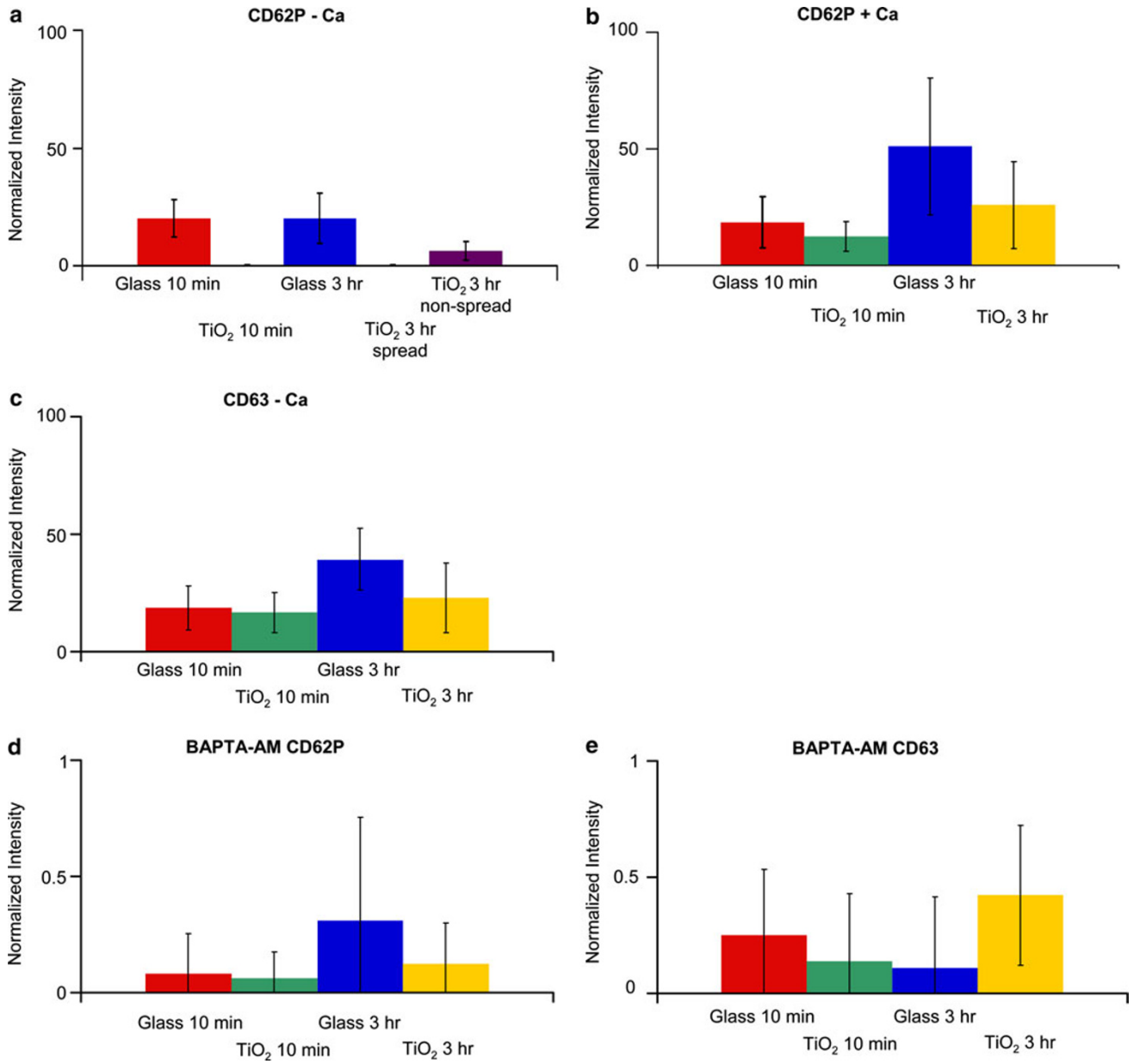

Fig. 4 Summary of the platelet activation profiles under different conditions employed in this study. Shown in this figure is the background-subtracted fluorescence intensity, $[(S - B)/B]$, where S is signal and B is background, in the *red* channel, corresponding to the expression of the activation markers CD62P or CD63 under different conditions used in this study. For each condition, the data was collected from at least three experiments using the blood of three different donors. The trends confirm those apparent in the individual images shown in Figs. 2 and 3. Note the change in scale: while in **a**–**c**, the fluorescence intensity is plotted on a scale from 0 to 100 %, in **d** and **e** it is plotted on the scale from 0 to 1 %, because the average intensity is so low under these conditions. **a** Expression of CD62P in platelets adhering on TiO_2 and on glass in the absence of Ca^{2+}. Significant levels of CD62P expression are seen on glass. On the other hand the expression is not detectable on TiO_2 after 10 min. After 3 h, the spread platelets do not express CD62P on TiO_2, while the non-spread platelets do express some. **b** Expression of CD62P in platelets adhering on TiO_2 and on glass in the presence of Ca^{2+}. CD62P is expressed on platelets adhering on both surfaces after 10 min and after 3 h. **c** Platelets express CD63 in the absence of Ca^{2+} on both surfaces. **d**, **e** Chelation of intracellular Ca^{2+} by BAPTA-AM affects the expression of both activation markers. Note the change in scale compared to **a**–**c**

4.2 Platelet Preparation [53, 81]

All procedures involving dispensing, pipetting, and transferring blood were carried out in a sterile laminar flow cabinet (Faster Two 30, Faster, Italy) to avoid contamination. Glass- and plasticware was autoclaved before use unless it was already sterile when purchased. Citrate-anticoagulated whole blood was transferred from the

Vacutainers to 1.5 ml Eppendorf Safe-lock microcentrifuge tubes (Sigma Aldrich, Madrid). Platelet count was determined with a ABX Micros 60 hematology analyzer (Horiba ABX Diagnostics, Madrid, Spain) and was typically in the range 1.5–2.5 $\times$ 10^8 platelets per ml. Platelet-rich plasma was prepared from whole blood by centrifugation at 600 rpm ($37\times g$) for 20 min at 37 °C in a 5417R Eppendorf centrifuge (Hamburg, Germany) equipped with a fixed angle rotor. At this point, platelet and other cell counts were measured with the hematology analyzer. Red and white blood cell counts were below 0.01 $\times$ 10^6 and below 0.1 $\times$ 10^6 cells per ml, respectively, platelet counts were on the order of 2.8 $\times$ 10^8 cells per ml.

PRP layers were collected into a 15 ml falcon tube and acid-citrate-dextrose (ACD; Sigma, Madrid, Spain) was added to the PRP in a ratio 1:6 by volume. Platelets were incubated for 10 min at 37 °C and then centrifuged at $700\times g$ at 22 °C for 20 min (Sigma 3K30 centrifuge, Fisher Scientific, fixed angle rotor). The pellet was re-suspended in citrate buffer (100 mM NaCl, 5 mM KCl, 5 mM Glucose, 1 mM $MgCl_2$, 15 mM citrate, pH 6.5) and centrifuged again at $700\times g$ at 22 °C for 10 min. The pellet was finally suspended in the HEPES isolation buffer (145 mM NaCl, 5 mM Glucose, 1 mM $MgCl_2$, 10 mM HEPES, 5 mM KCl, pH 7.4). For experiments to be carried out in the presence of extracellular calcium, the pellet was re-suspended in the HEPES isolation buffer containing 2 mM calcium. Platelet concentration was adjusted to $\sim$1 $\times$ 10^8 cells per ml. Platelet purity was ascertained by flow cytometry (described below) and was found to be above 99 %.

Protein concentration in the purified platelets was measured with an ND-1000 Nanodrop spectrophotometer system (Wilmington, DE, USA) using an extinction coefficient of $\sim$1 ml g^{-1} cm^{-1}.

Platelet isolation was performed within $\sim$12 h of blood collection. All experiments were completed within 24 h of blood collection. Each experiment was carried out at least three times with blood from three different donors.

4.3 Platelet analysis by flow cytometry [33, 53, 56, 82, 83]

Flow cytometry was performed on freshly isolated platelets to analyze their purity, basal activity, and response to agonists, with a FACScalibur Flow cytometer (Becton–Dickinson, Madrid, Spain). 50 µl of the washed platelets were mixed with 50 µl of HEPES calcium-free buffer or with 2 mM calcium buffer, as required. For stimulating platelets, either TRAP (Thrombin receptor activating peptide, Sigma-Aldrich, Madrid, Spain) at a final concentration of 70 µM, or PMA (Phorbyl methyl acetate, Sigma-Aldrich, Madrid, Spain), at a final concentration of 10 µM, were added to the samples. Platelets were identified by staining samples with PerCPCy5.5-conjugated anti-CD41a antibody. Activation was evaluated by staining them with PE-conjugated anti-CD62P (P-selectin), PE-conjugated anti-CD63, FITC-conjugated PAC1 (antibody against the active conformation of GPIIb/IIIa) and APC-conjugated Annexin A5 (staining agent for phosphatidyl serine, PS), in separate tubes. All the fluorescently labeled reagents used in the flow cytometry experiments were purchased from Becton–Dickinson, Madrid, Spain. Samples were incubated for 30 min at 37 °C without agitation before being diluted with 2 ml of the respective buffer and analyzed by flow cytometry. Isotype-matched controls were run in parallel to all monoclonal antibodies. Light scatter and fluorescence data from 10,000 events were collected with all the detectors in the logarithmic mode. Antibody binding was expressed as percentage of platelets positive for an antibody using Flow Jo software (Tree Star Inc, Oregon, USA).

4.4 Surface Preparation and Cleaning

Surfaces used in this study were either bare 25 mm #1 microscope coverslip glass slides (Menzel-Gläser, Braunschweig, Germany), or the same glass slides coated with $\sim$20 nm layer of TiO_2 by magnetron reactive sputtering. The coating was done in a Leybold dc-magnetron Z600 sputtering unit at the Paul Scherrer Institut (Villigen, Switzerland) according to the previously published protocol [84].

Immediately prior to each experiment, surfaces were cleaned in 2 % SDS solution that was filtered through 0.2 µm pore diameter syringe filter for 30 min, washed under a stream of Nano-pure water (Nanopure Diamond^{TM}, Barnstead International, USA), dried with a stream of filtered nitrogen gas (99.999, AirLiquide Spain, Derio, Spain), and further cleaned for 30 min in a UV-Ozone cleaner (BioForce Nanosciences, USA) that was pre-heated for 30 min immediately prior to this step. This procedure results in minimal carbon contamination of the surface (<10 %) as judged by XPS (SAGE HR100, Specs, Berlin, Germany). No other impurities were detected on the surfaces cleaned in this way. This cleaning procedure has been used by several groups for a wide variety of biophysical studies [8, 14, 15, 85].

4.5 Platelet Adhesion and Activation Studies on Glass and TiO_2 Surfaces

Platelet adhesion experiments were started no later than 2 h after platelet preparation. The entire experiment was performed at 37 °C.

Freshly cleaned surfaces were mounted in home-made, 500 µl hollow Teflon cells using dental glue. 250 µl of the

buffer required for the experiment was added to the cell immediately after the glue had set (~2 min) to reduce as much as possible the chances of contaminating the surface, followed by 250 µl of the washed platelets in the same buffer, and incubated either for 10 min or for 3 h.

After the incubation, the samples were washed by adding and withdrawing 250 µl of the buffer 20× to remove any non-adhered platelets. Care was taken not to touch the surface with the pipette tip, not to introduce bubbles, and not to dry the sample out.

Washed samples were incubated with 5 µl of PerCPCy5.5 anti-CD41a antibody and with PE anti-CD62P or PE anti-CD63 antibody for 30 min and analyzed using confocal microscope (see below).

For experiments involving platelet stimulation with an agonist, the above steps were followed by the addition of TRAP to the sample cell, incubation for 30 min, and confocal microscopy analysis. For experiments involving intracellular calcium chelation with BAPTA-AM, platelets were isolated in calcium free buffer and incubated in the presence the desired BAPTA-AM concentration (1, 2, 5, 8, 10, 100 µM) for 30 min before they were treated with an agonist (TRAP) in solution or allowed to interact with the surfaces. The results of solution experiments are shown in Fig. 3b, and the results of the surface experiments are shown in Fig. 3c.

4.6 Confocal Microscopy and Image Analysis

Fluorescence images were obtained using an LSM 510 confocal laser scanning microscope (Carl Zeiss, Jena, Germany) equipped with Plan-Apochromat 63×/1.40 NA oil immersion objective. All experiments were carried out in a temperature controlled stage at 37 °C. PerCP Cy5.5 and PE fluorescence was excited with the 488 nm line of the Ar laser and detected with an avalanche photodiode and a photomultiplier with LP 655 and BP575-615IR filters, respectively. 143 × 143 µm^2 512 × 512 or 2,048 × 2,048 pixel images were recorded and analyzed using the Zen (Carl Zeiss, Jena, Germany) or ImageJ version 1.42 software to extract the numbers and sizes of the adhering platelets as well as to highlight the different types of platelets observed on the surface. The image analysis procedure was as follows. First, the multi-channel images were split into separate channels—one corresponding to the anti-CD41a fluorescence and one corresponding to the CD62P or CD63 fluorescence. Second, a Gaussian blur filter was applied to both sets of images to highlight platelet edges.

The numbers of adhering platelets were quantified using the ImageJ cell counter plugin. Platelets adhering on the surfaces for 3 h were counted manually because cells were overlapping and it was difficult to separate them. The numbers of adhering platelets are quoted in Table S3.

Platelet areas were measured manually by drawing regions of interest around the platelets using the free hand drawing tool. Based on the analysis of 180 cells, radii were calculated to determine the size distribution of the platelets, adhered on the surface for different experiment conditions. Due to the aggregation of platelets after 3 h, the exact number and size of adhered platelets were difficult to quantify. The results of these analyses under different experimental conditions are shown in Figure S3.

Two methods were used to determine which of the adhering platelets were activated:

Method I: First, blurred images for the CD41a and CD62P or CD63 channel were false colored green and red respectively. Co-localization was visualized in the merged images in terms of the appearance of the yellow color. These images are shown in Figs. 2 and 3 in and Figure S4 in the Supporting Information.

Method II: Background subtraction with rolling ball radius 50 was used to separate the fluorescence coming from the spread and the non-spread platelets in each channel (see white circles in Fig. 2a). The resulting background-subtracted images were thresholded, leading to binary images. Logical AND operation was used in the binary images from each channel to obtain the outline image shown in Fig. 2a-vii. In such an image, the co-localization of the two dyes (anti-CD41a and anti-CD62P, green and red channels, respectively), appears as a double boundary, signaling activated platelets. Non-activated platelets appear as single boundaries.

Interestingly, it was the non-spread platelets that were activated, as shown by both methods. See Sects. 2 and 3 for further explanation.

To calculate the background subtracted average fluorescence intensities shown in Fig. 4, individual cells were selected in ImageJ and median intensity within the selected region in the red channel was calculated. Median intensities for regions where there were no cells were measured as well. The intensity for each cell in a given image was than normalized by the background intensity $I = [(I(cell) - I(background)]/I(background)$. These normalized intensities were averaged over the cells observed in different experiments performed under nominally the same experimental conditions but with blood taken from different donors. The results are plotted in Fig. 4.

4.7 Cell Viability Analysis [86]

Membrane integrity in platelets adhering on the bare glass and TiO2-coated glass surfaces was measured by Calcein-AM stain. This marker is retained in the cytoplasm and degraded by esterases, unless the cell membrane is damaged. After the adhesion of cells on the surface for 10 min and 3 h, they were washed, and then 200 µl of 2 mM

Calcein-AM solution was added to the surface. After staining for 30 min at 37 °C, labeled cells were visualized using confocal microscope. This analysis showed that adhesion to the surface did not affect the integrity of the platelet membranes.

Acknowledgments We would like to acknowledge funding from the Department of Industry of the Basque Government (program ETORTEK) and from the Spanish Ministry of Science and Innovation (MICINN, ref. CTQ2009-11245) to I.R.; Michael Horisberger (Paul Scherrer Institut, Villigen, Switzerland) is gratefully acknowledged for TiO_2-coated glass slides; Drs. Laura Saa and Valeri Pavlov allowing us to use their centrifuge and Nanodrop equipment; Drs. Jose Manuel Cardenas Diaz De Espada, Roberto Bilbao Urquiola, Amaia del Villar Álvarez, and Ms. Clara Rodriuez Aierbe (Basque Biobank for Research, Galdakao, Spain); Ms. Mari Carmen Pozo and Dr. Mari Mar Lertxundi (Basque Biobank for Research, San Sebastian, Spain) for organizing the blood collection and testing.

References

1. Kasemo B (2002) Surf Sci 500:656–677
2. Brunette DM, Tengvall P, Textor M, Thomsen P (2001) Titanium in Medicine. Springer, Berlin
3. Kasemo B (1983) J Prosthet Dent 49:832–837
4. Parsegian VA (1983) J Prosthet Dent 49:838–842
5. Purcell G, Sun SC (1963) Trans Am Inst Min Eng 226:6–12
6. Kosmulski M, Gustafsson J, Rosenholm JB (1999) Colloid Polym Sci 277:550–556
7. Kosmulski M (2002) Adv Colloid Interface Sci 99:255–264
8. Rossetti FF (2005) Thesis, Swiss Federal Institute of Technology
9. Lyklema J (2006) Colloids Surf Physicochem Eng Asp 291:3–12
10. Hunter R (2001) Foundations of Colloidal Science. Oxford University Press, Oxford
11. Ellingsen JE (1991) Biomaterials 12:593–596
12. Reviakine I, Gallego M, Camarero S, Lütgebaucks C, Wacklin HP (2012) Manuscript in preparation
13. Khan TR, Grandin HM, Mashaghi A, Textor M, Reimhult E, Reviakine I (2008) Biointerphases 3:FA90–FA95
14. Rossetti FF, Textor M, Reviakine I (2006) Langmuir 22:3467–3473
15. Rossetti FF, Bally M, Michel R, Textor M, Reviakine I (2005) Langmuir 21:6443–6450
16. Allen LH, Matijevi E (1969) J Colloid Interface Sci 31:287
17. Janusz W, Patkowski J, Chibowski S (2003) J Colloid Interface Sci 266:259–268
18. Eyre L, Gamlin F (2010) Anaesth Intensive Care Med 11:244–246
19. Whiteheart SW (2011) Blood 118:1190–1191
20. Michelson A (2007) In: Michelson (ed) Platelets, 2nd edn. Academic Press, London
21. Leslie M (2010) Science 328:562–564
22. Eppley BL, Pietrzak WS, Blanton M (2006) Plast Reconstr Surg 118:147E–159E
23. Solum NO (1999) Arterioscler Thromb Vasc Biol 19:2841–2846
24. Balasubramanian K, Schroit AJ (2003) Annu Rev Physiol 65:701–734
25. Mirlashari MR, Ryningen A, Mikkelsen HM, Fukami MH (1996) Platelets 7:313–320
26. Goodman SL, Cooper SL, Albrecht RM (1993) J Biomed Mater Res 27:683–695
27. Peerschke EIB (1995) Am J Pathol 147:678–687
28. Varga-Szabo D, Pleines I, Nieswandt B (2008) Arterioscler Thromb Vasc Biol 28:403–412
29. Sivaraman B, Latour RA (2011) Biomaterials 32:5365–5370
30. Broberg M, Eriksson C, Nygren H (2002) J Lab Clin Med 139:163–172
31. Patel D, Vaananen H, Jirouskova M, Hoffmann T, Bodian C, Coller BS (2003) Blood 101:929–936
32. Michelson A (1996) Blood 87:4925–4936
33. Michelson AD, Furman MI (1999) Curr Opin Hematol 6:342–348
34. Gorbet MB, Sefton MV (2004) Biomaterials 25:5681–5703
35. Ratner BD (2007) Biomaterials 28:5144–5147
36. Haycox CL, Ratner BD (1993) J Biomed Mater Res 27:1181–1193
37. Rhodes NP, Zuzel M, Williams DF, Derrick MR (1994) J Biomed Mater Res 28:435–439
38. Andersson M, Sellborn A, Fant C, Gretzer C, Elwing H (2002) J Biomater Sci Polym Edit 13:907–917
39. Kang IK, Ito Y, Sisido M, Imanishi Y (1988) J Biomed Mater Res 22:595–611
40. Hansson KM, Tosatti S, Isaksson J, Wettero J, Textor M, Lindahl TL, Tengvall P (2005) Biomaterials 26:861–872
41. Kanagaraja S, Lundstrom I, Nygren H, Tengvall P (1996) Biomaterials 17:2225–2232
42. Nygren H, Tengvall P, Lundstrom I (1997) J Biomed Mater Res 34:487–492
43. Hong J, Andersson J, Ekdahl KN, Elgue G, Axen N, Larsson R, Nilsson B (1999) Thromb Haemost 82:58–64
44. Jones MI, McColl IR, Grant DM, Parker KG, Parker TL (2000) J Biomed Mater Res 52:413–421
45. Huang N, Yang P, Leng YX, Chen JY, Sun H, Wang J, Wang GJ, Ding PD, Xi TF, Leng Y (2003) Biomaterials 24:2177–2187
46. Takemoto S, Yamamoto T, Tsuru K, Hayakawa S, Osaka A (2004). In: Bioceramics, vol 16(254-2), pp 853–856
47. Maitz MF, Pham MT, Wieser E, Tsyganov I (2003) J Biomater Appl 17:303–319
48. Park JY, Gemmelll CH, Davies JE (2001) Biomaterials 22:2671–2682
49. Park JY, Davies JE (2000) Clin Oral Implant Res 11:530–539
50. Kikuchi L, Park JY, Victor C, Davies JE (2005) Biomaterials 26:5285–5295
51. Tsyganov I, Maitz MF, Wieser E, Richter E, Reuther H (2005) Surf Coat Technol 200:1041–1044
52. Nonckreman CJ, Fleith S, Rouxhet PG, Dupont-Gillain CC (2011) Colloids Surf B Biointerfaces 77:139–149
53. Watson SP (1996) Platelets: a practical approach. Oxford University Press, USA
54. Shattil SJ, Hoxie JA, Cunningham M, Brass LF (1985) J Biol Chem 260:1107–1114
55. Michelson AD, Linden MD, Barnard MR, Furman MI, Frelinger AL III (2007) In: Michelson AD (ed) Platelets, 2nd edn. Academic Press, London
56. Hagberg IA, Lyberg T (2000) Platelets 11:137–150
57. Flaumenhaft R, Dilks JR, Rozenvayn N, Monahan-Earley RA, Feng D, Dvorak AM (2005) Blood 105:3879–3887
58. Hu H, Forslund M, Li N (2005) Thromb Res 116:241–247
59. Meers P (1996). In: Seaton BA (ed) Annexins: molecular structure to cellular function, pp 97–119
60. White GC 2nd, Scarborough DE, Brinkhous KM (1983) Ann N Y Acad Sci 416:351–362

61. Hartwig JH (2007) In: Michelson AD (ed) Platelets. Academic Press, London, pp 75–97
62. Fritz M, Radmacher M, Gaub HE (1994) Biophys J 66: 1328–1334
63. Ariyoshi H, Salzman EW (1996) Arterioscler Thromb Vasc Biol 16:230–235
64. Wencel-Drake JD, Plow EF, Kunicki TJ, Woods VL, Keller DM, Ginsberg MH (1986) Am J Pathol 124:324–334
65. Tsien RY (1980) Biochemistry 19:2396–2404
66. Davies TA, Drotts DL, Weil GJ, Simons ER (1989) J Biol Chem 264:19600–19606
67. Carretero M, Diaz-Ricart M, Fuste B, Estebanell E, Escolar G, Ordinas A (2002) Platelets 13:77–83
68. Golanski J, Pietrucha T, Baj Z, Greger J, Watala C (1996) Thromb Res 83:199–216
69. Schneider DJ, Tracy PB, Mann KG, Sobel BE (1997) Circulation 96:2877–2883
70. Li Z, Delaney MK, O'Brien KA, Du X (2011) Arterioscler Thromb Vasc Biol 30:2341–2349
71. Cerecedo D, Stock R, Gonzalez S, Reyes E, Mondragon R (2002) Haematologica 87:1165–1176
72. Broberg M, Nygren H (1998) Colloids Surfaces B Biointerfaces 11:67–77
73. Pandey D, Goyal P, Siess W (2007) Blood Cells Mol Dis 38:269–279
74. Taylor ML, Misso NLA, Stewart GA, Thompson PJ (1995) Platelets 6:394–401
75. Shirakawa R, Yoshioka A, Horiuchi H, Nishioka H, Tabuchi A, Kita T (2000) J Biol Chem 275:33844–33849
76. Fukuda M (2008) Cell Mol Life Sci 65:2801–2813
77. Tolmachova T, Abrink M, Futter CE, Authi KS, Seabra MC (2007) Proc Natl Acad Sci USA 104:5872–5877
78. Yoshioka A, Horiuchi H, Shirakawa R, Nishioka H, Tabuchi A, Higashi T, Yamamoto A, Kita T (2001) Atherosclerosis Vi 947:403–406
79. Italiano JE Jr, Battinelli EM (2009) J Thromb Haemost 7: 173–176
80. Verheul HM, Lolkema MP, Qian DZ, Hilkes YH, Liapi E, Akkerman JW, Pili R, Voest EE (2007) Clin Cancer Res 13:5341–5347
81. van der Zee PM, Biro E, Ko Y, de Winter RJ, Hack CE, Sturk A, Nieuwland R (2006) Clin Chem 52:657–664
82. Tomer A (2004) J Biol Regul Homeost Agents 18:172–177
83. Shattil SJ, Cunningham M, Hoxie JA (1987) Blood 70:307–315
84. Kurrat R, Textor M, Ramsden JJ, Boni P, Spencer ND (1997) Rev Sci Instrum 68:2172–2176
85. Reviakine I, Rossetti FF, Morozov AN, Textor M (2005) J Chem Phys 122:204711–204718
86. Gibbins JM, Mahaut-Smith MP (eds) (2010) Platelets and megakaryocytes: functional assays. In: Methods in molecular biology, vol 1. Human Press, New Jersey